JMEPEG (2012) 21:2274–2282
DOI: 10.1007/s11665-012-0170-y
©ASM International
1059-9495/$19.00

Erosion and Corrosion Behavior of Laser Cladded Stainless Steels with Tungsten Carbide

Raghuvir Singh, Mukesh Kumar, Deepak Kumar, and Suman K. Mishra

(Submitted December 15, 2011; in revised form January 6, 2012)

Laser cladding of tungsten carbide (WC) on stainless steels 13Cr-4Ni and AISI 304 substrates has been performed using high power diode laser. The cladded stainless steels were characterized for microstructural changes, hardness, solid particle erosion resistance and corrosion behavior. Resistance of the clad to solid particle erosion was evaluated using alumina particles according to ASTM G76 and corrosion behavior was studied by employing the anodic polarization and open circuit potential measurement in 3.5% NaCl solution and tap water. The hardness of laser cladded AISI 304 and 13Cr-4Ni stainless steel was increased up to 815 and 725$Hv_{100\ g}$, respectively. The erosion resistance of the modified surface was improved significantly such that the erosion rate of cladded AISI 304 (at 114 W/mm^2) was observed ~0.74 mg/cm^2/h as compared to ~1.16 and 0.97 mg/cm^2/h for untreated AISI 304 and 13Cr-4Ni, respectively. Laser cladding of both the stainless steels, however, reduced the corrosion resistance in both NaCl and tap water.

Keywords corrosion, erosion, hydro turbine, laser cladding, stainless steel 13Cr-4Ni and AISI 304, tungsten carbide

1. Introduction

Stainless steels are widely used to fabricate the components of hydro turbines as they posses good mechanical and corrosion resistance properties. They, however, undergo severe erosion and corrosive-wear during operation. For instances, after about 6000-8000 h of operation, turbine blade (under optimal loads) lost ~40-60 kg of metal due to erosion (Ref 1). Martensitic and austenitic stainless steels are the most popular choices for runner blades, guide vanes, and labyrinth (rotating) seal. The martensitic stainless steels possess higher erosion resistance than the austenitic stainless steels while the ferritic stainless steels have the lowest cavitation erosion resistance (Ref 2). Despite great amount of work has been done on the development of material and hydro turbine design, the problem of silt cavitation/erosion is yet remained unsolved.

Erosion and cavitation, being surface phenomenon, are possible to overcome largely by modifying and tailoring the surface to suit specific environment (Ref 3). Several surface treatment methodologies and coating systems such as borides, nitrides, and carbides have been employed on the components of hydropower plants. Graham et al. (Ref 4) reported better erosion resistance of the boron carbide (B_4C) than the tungsten carbide/cobalt coating whereas the WC-Co exhibited better abrasion resistance due to its higher toughness than the boron carbide coating. A combination of hardness and toughness generally yields superior performance against both erosion and abrasion. Mann et al. (Ref 5) showed WC coating applied by HVOF process on the martensitic stainless steel failed to improve the erosion resistance during droplet erosion. The coating was delaminated in a layer-wise manner during the test. Toma et al. (Ref 6) fabricated various cermet coatings such as WC and Cr_3C_2 in combination with Co, Cr, and Ni matrix, using HVOF process, on the high alloyed steel (1.457). They showed WC-Co the least whereas Cr_3C_2-NiCr the highest erosion-corrosion resistant, primarily due to NiCr being a better corrosion resistant matrix than the Co.

Laser surface cladding is relatively a newer engineering technique to produce metallurgically bonded coating for industrial applications (Ref 7). It gives high cooling rates (~10^3-10^6 K/s) such that the metastable phases can be evolved due to a non-equilibrium processing. Various alloys and ceramic powders have been tried to deposit on the surface of different engineering alloys using high power lasers. Tungsten carbide cladding among ceramics has been cladded on the surface of steel substrates by several researchers and shown to improve hardness and wear resistance to different extents. Preliminary study made by Cheng et.al (Ref 8) showed improvement in the cavitation resistance of AISI 316 stainless steel by cladding (using CO_2 and Nd-YAG laser) the pre-placed ceramic powders of various compositions. They compared the performance of WC, Cr_3C_2, SiC, TiC, CrB_2, and Cr_2O_3 and found CrB_2 and WC relatively better than the others. Cr_2O_3 did not improve the erosion resistance. A high hardness and indentation recovery ratio have been attributed to the better erosion resistance of CrB_2 and WC (Ref 8). Wu et al. (Ref 9) fabricated a gradient nickel-based WC cladding to reduce the stress concentration and crack formation in steel substrate. Three clad layers were laid by varying the process parameters so that the WC concentration gradually changes toward an outer surface. Such cladding did not appear useful for long-term wear applications due to poor interfacial bonding between WC

Electronic supplementary material The online version of this article (doi:10.1007/s11665-012-0170-y) contains supplementary material, which is available to authorized users.

Raghuvir Singh, Mukesh Kumar, Deepak Kumar, and **Suman K. Mishra**, CSIR-National Metallurgical Laboratory, Jamshedpur 831007, India. Contact e-mails: raghujog@yahoo.co.in and rsr@nmlindia.org.

and the substrate. Riabkina-Fishman et al. (Ref 10) produced functionally graded WC cladding, on tool steel by varying the composition of W and C in the range 12-58 wt.% and 1.3-4.3 wt.%, respectively. Tungsten was noticed to increase in a layer-wise manner up to 75% on the outermost layer. A very high hardness ~1600 HV on the top layer was thus produced (Ref 10). Przybyłowicz et al. (Ref 11) performed microstructural study of laser cladded WC steel and noticed that the long interaction time between laser beam materials increased the dissolution of primary carbides and thus reduced the hardness. A pulse Nd-YAG laser cladding of WC-12 wt.% Co was fabricated on a low carbon steel to study the interphase strength and hardness (Ref 12). This produced adhesion (interphase) strength ~60 MPa and microhardness ~1350 HV. Yang et al (Ref 13) produced cladding with powder contained different compositions of W, C, Co, and WC on carbon steel, using high power CO_2 laser, and analyzed various phases evolved. Zhong et al. (Ref 14) studied the morphology and growth of WC crystal along with the phase evolution in WC/Ni cladded steel. They observed WC, CW_3, WNi, FeW_3C, Fe_6W_6C, W_3O, W, C, and (Fe,Ni) phases in the clad. Nickel and cobalt-based WC cladding were produced by Hidouci et al. (Ref 15) on steel substrate using continuous CO_2 laser. Higher hardness of Co based than the Ni-based WC cladding was noticed. A Co-based WC produced cellular and dendritic while Ni-based showed homogeneous microstructure. The influence of size of WC/W_2C particles cladding on wear behavior of low carbon steel was investigated; finer the particles better the wear resistance was observed (Ref 16). A nickel-based self-reflexing coating reinforced with a mixture of conventional and nanostructured WC-Co (30%) showed very low wear rates (Ref 17).

While literature indicates immense potential in WC cladding (using high power laser) to improve various surface properties, erosion, and corrosion of WC modified surfaces has rarely been attempted. The most findings have been focused on the microstructural investigation, hardness, and sliding wear characterization of laser cladded surfaces. Since severe erosion, cavitation, and corrosion are the predominate reasons of failure of components in hydropower plants, WC cladding should be evaluated for erosion, cavitation, and corrosion. A few have attempted cavitation resistance of WC modified surfaces (Ref 8) by using 20 kHz ultrasonic vibrator which involves vibration induced cavitation. One of the major causes of erosion in the hydraulic machineries is silt (hardness ~1200 HV) that ranges between 5000 and 20,000 ppm in river water; this promotes wear and fatigue of the components of turbine. Nanda et al. (Ref 18) reported that the medium silt content causes 4 times higher erosion than the cavitation in clean water (without silt) and the combined effect of cavitation and erosion is 16 times higher than the cavitation alone. It is, thus, necessary to study the WC cladding against hard particle erosion and corrosion resistance of the cladded surface. This article discusses the results on the laser cladding of tungesten carbide (83WC-17Co) on 13Cr-4Ni and AISI 304 stainless steels obtained by using high power diode laser (HPDL). The microstructural, erosion, and corrosion behavior of laser cladded steels have been investigated.

2. Experimental Procedures

Stainless steel 13Cr-4Ni and AISI 304 were chosen as substrate materials, as they are used for hydropower plants and suffer from severe erosion and cavitation losses. Tungsten carbide (83WC/17Co supplied by H.C. Starck, GmbH Germany) was used as a precursor material applied on the surface of stainless steels 13Cr-4Ni and AISI 304. A mean particle size of tungsten carbide powders (of globular morphology) was ~45.6 μm and varied in the range 20-65 μm. HPDL (supplied by M/s SIL Pune, India) was used for the cladding of tungsten carbide on stainless steels at a different output energy and beam size ~4.1 mm (using optics of focal length ~166 mm). The laser powers >114 W/mm^2 were chosen for cladding as the powder cladded at below 114 W/mm^2 and scan speed of 600 mm/min remained loose on the surface of stainless steel. Laser tracks were laid at ~25% overlapping. The WC powders were fed using a feeder (supplied by GTV, Germany). The powder aligned with the laser beam using a co-axial cladding head was focused on the surface of the specimen. Single track, before multiple scanning, at different operating parameters were laid to see the physical appearance of cladding. Various process parameters used during cladding are listed in Table 1.

For microstructural investigation, cross section of the clads were mounted using bakelite powder, ground and polished on emery papers (of the grit size ranging from 220 to 1200) followed by cloth polishing using alumina slurry containing ~0.05 μm alumina particles. Specimens were then etched with an aquaregia, a mixture of concentrated nitric acid and hydrochloric acid in the ratio of 1:3. Both untreated and laser cladded specimens were viewed under the scanning electron microscope (SEM) (Hitachi S 3400N make). Phase identification was carried out using Seifert 3003 PTS X-ray diffractometer with Co Kα radiations. Hardness on the cross section at a varied distance from the outermost surface of the laser cladded stainless steels was determined by the microhardness tester (Leica VMHT auto, GMBH Austria). The average of eight indents, at each distance from the outer surface, was reported as a mean hardness value.

The solid particle erosion was carried out according to the method prescribed in ASTM standard G76-07 (Standard Test Method for Conducting Erosion Tests by Solid Particle Impingement Using Gas Jets). Various parameters used for the erosion tests were: nozzle diameter ~2.8 mm, particle discharge speed ~9.8 m/s, and particle size of the erodent (alumina) ~150 μm. All the specimens were placed at an angle of 30° with respect to the nozzle axis. Erosion and corrosion experiments were made on AISI 304 only as cladded surface has been the subject of study and substrate (both being stainless steels) is not expected to change the clad properties. The results, however, have been compared with the both untreated 13Cr-4Ni and AISI 304 stainless steels.

Corrosion behavior of laser cladded and untreated substrates was evaluated using an open circuit potential (OCP) versus time, anodic polarization, and tafel plots using Reference 600 potentiostat (Gamry Instruments USA make). The tafel plots

Table 1 Laser operating parameters cladding stainless steel

Laser power density, W/mm^2	Scan speed, mm/min	Powder feed rate, g/s
114 144 159 182	600	16

and anodic polarization curves were recorded by sweeping the potential from −100 mV (with respect to OCP) in the noble direction at a constant scan rate of 1 mV/s. For tafel plots, the specimens were scanned within ±250 mV with respect to OCP of the specimen. Saturated calomel electrode (SCE) was used as a reference and graphite as a counter electrode. All the electrochemical tests were conducted in the tap water containing (ppm) Cl^-—49.7, SO_4^{2-}—42, and CO_3^{2-}—100 (pH 7.09) and 3.5% NaCl solution. The tap water simulates the river water conditions where components of hydropower plants are actually exposed.

3. Result and Discussions

3.1 Microstructural and Mechanical Characterization

A few clad morphologies (cross section of laser clad) obtained at a different laser parameters, e.g., 114 and 144 W/mm^2 are shown in Fig. 1. The aspect ratio (maximum depth to width) of clad zone was found to vary with laser power density. Increase in the laser power density from 114 to 182 W/mm^2 enhanced the aspect ratio of clad from 0.461 to 0.769 μm and 0.396 to 0.734 μm on AISI 304 and 13Cr-4Ni, respectively. By knowing the aspect ratio, overlapping of the laser tracks on the surface can be estimated for optimum utilization of the laser energy. Increase in the laser power density increases the temperature of the substrate and results in larger quantity of molten volume (include fed powder and substrate). A slightly larger molten volume on the surface of AISI 304 as compared to 13Cr-4Ni was noticed. This may be due to the difference in the absorptivity of the two stainless steels to the diode lasers. The clad region in both the stainless steel shows a complex microstructure consisting of cellular, dendrite, columnar, and elongated grains with varied dendrite arms. Tungsten carbide particles and network of the eutectic carbides along the grain boundaries in both the stainless steels 13Cr-4Ni and AISI 304 are shown in Fig. 2. The whiter regions are noticed to be richer in tungsten (W) as compared to the others, e.g., gray regions. Bulk analysis (SEM-EDAX) shows approximately 20-24% (by wt.) tungsten on the laser cladded surface. The qualitative SEM line profile analysis across the clad thickness presented in Fig. 3 indicates decrease in tungsten concentration after the remelted/interface region towards the base. Presence of WC as a main phase along with W_3C, and W_2C as minor phases were found on the clad surface by XRD analysis. A similar observation has been reported by earlier researchers (Ref 8).

The microhardness profile for laser cladded AISI 304 and 13Cr-4Ni is shown in Fig. 4. The hardness of 13Cr-4Ni and AISI 304 was found to increase by more than 2.5 and 3 times, respectively. It was found to reduce abruptly at the interphase of AISI 304 as compared to that of 13Cr-4Ni which is possibly due to the evolution of sharp interphase boundary in AISI 304 than in the 13Cr-4Ni, as illustrated in Fig. 5. The latter shows a gradation in the microstructure near the interphase zone.

3.2 Erosion Behavior

The cumulative weight loss obtained for stainless steels during solid particle jet erosion test, conducted for 40 h, is shown in Fig. 6(a). The performance of laser cladded specimens were compared with the results obtained from HVOF coating (tungsten carbide) and the base substrates. Marked difference in the weight loss of laser treated and untreated stainless steel is apparent from the figure. Both AISI 304 and 13Cr-4Ni without cladding suffered from higher erosion as compared to that of their cladded counterparts. Until ∼10 h of exposure, weight loss of all the specimens remained almost similar but differs with further increase in the time. The erosion loss of HVOF coated stainless steel is significantly higher than that of the untreated and cladded substrates. This could be due to the poor adhesion and porous nature of the coating. Similar observation on higher erosion loss of HVOF coated (with NiCr and Stellite) boiler tube than the base substrate has been made by the earlier researchers (Ref 19). Two different slopes ∼4.5 and 1.5 in the mass loss versus time plot (presented in Fig. 6) for HVOF coated specimen exhibit a change in the erosion kinetics. The first slope (∼4.5) indicates the erosion damage of WC coating which detached after ∼10 h of erosion; on further exposure of the heat affected/alloyed zone (next to WC clad) in the base substrate yielded a different erosion rate and slope (∼1.5). The slope of weight loss versus time plot of specimen laser cladded at 114 W/mm^2 is ∼1.0. The erosion rates (obtained by converting the mass loss) were plotted (versus time) and presented in Fig. 6(b). Figure shows that the erosion rate of stainless steels, both with and without laser cladding, becomes almost constant after 4-5 h of exposure; AISI 304 and

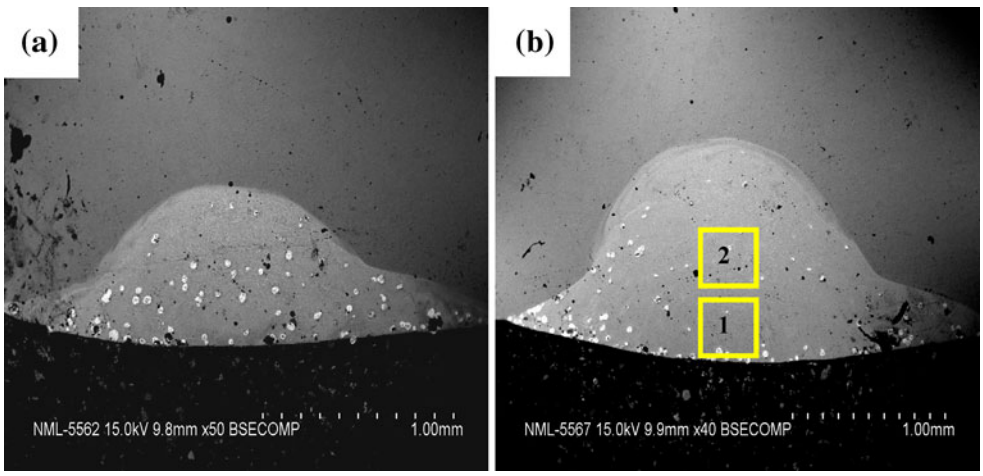

Fig. 1 Cross section view of laser track on stainless steel 13-4 (a) 114 and (b) 144 W/mm^2

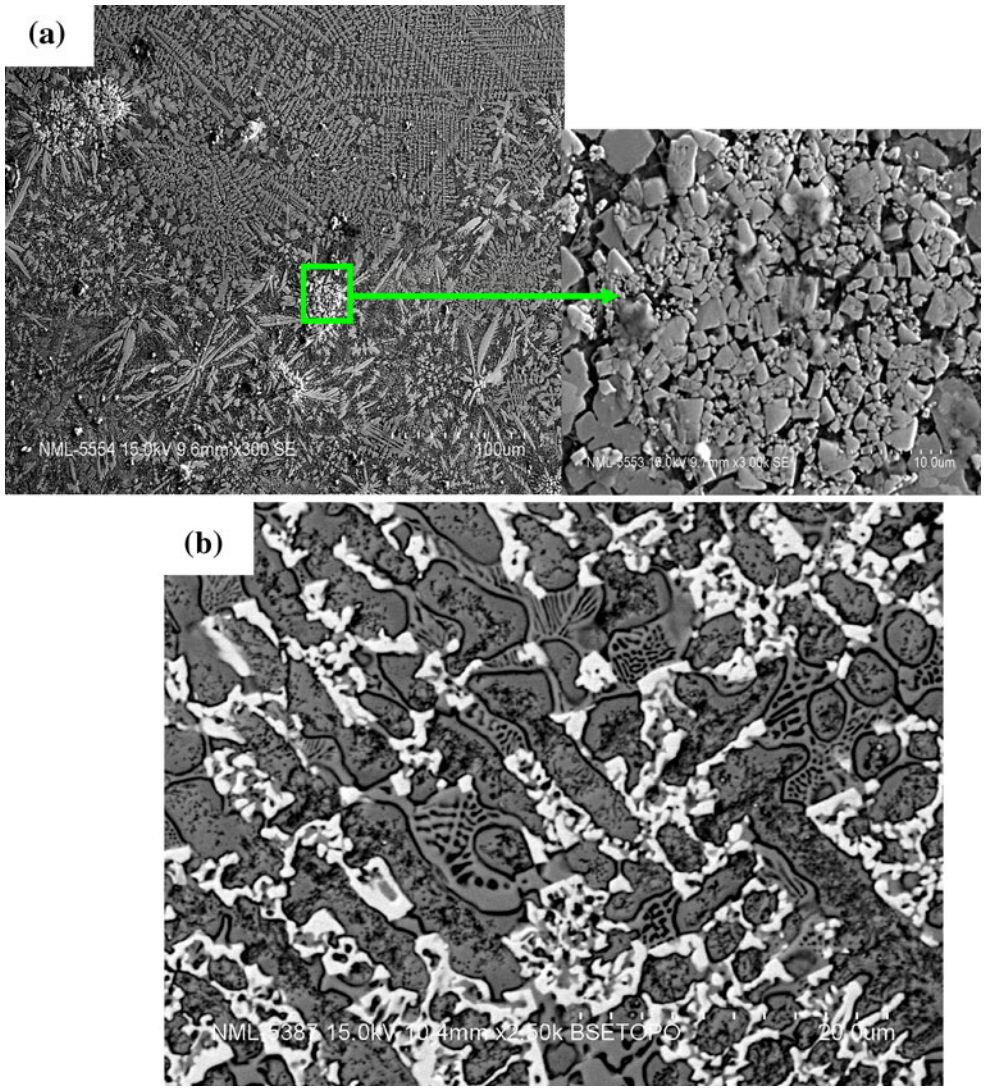

Fig. 2 Microstructural variations in the laser clad regions (at 114 W/mm^2) as indicated in Fig. 1(b): (a) dendrites and tungsten carbide particles near the top surface (b) cellular region containing eutectic carbides

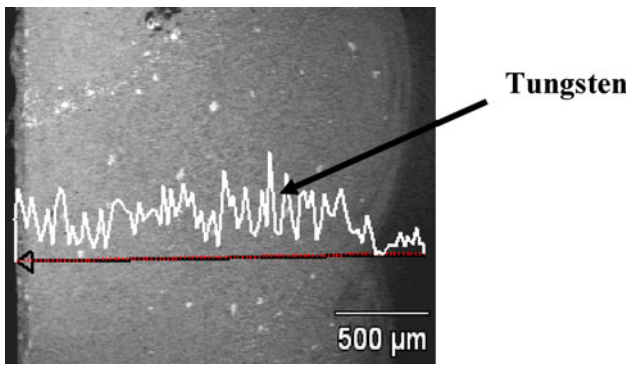

Fig. 3 Qualitative line profile across the clad thickness of laser cladded stainless steel at 114 W/mm^2

13Cr-4Ni shows erosion rate ~1.16 and 0.97 mg/cm^2/h after 40 h. Laser cladded stainless steels show lower erosion as compared to the base substrate; it is ~0.74 mg/cm^2/h for laser

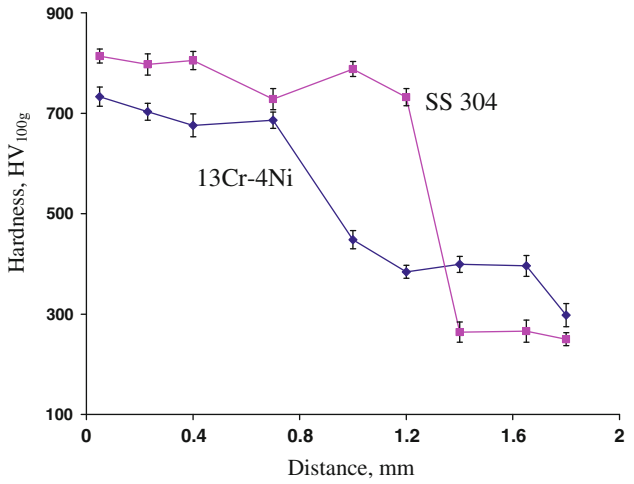

Fig. 4 Variation in microhardness of laser cladded AISI 304 and 13Cr-4Ni stainless steels at 144 W/mm^2 laser power density

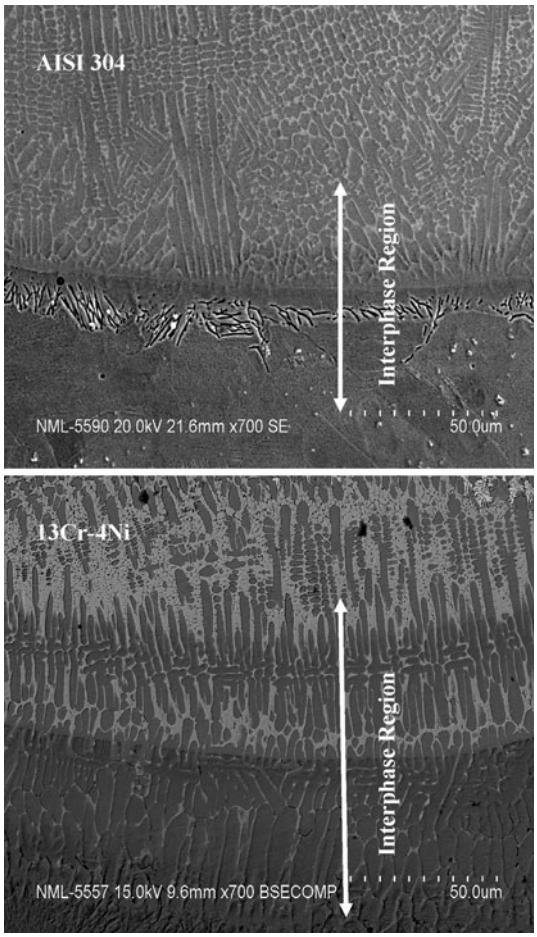

Fig. 5 Difference in interphase region of AISI 304 and 13Cr-4Ni stainless steel

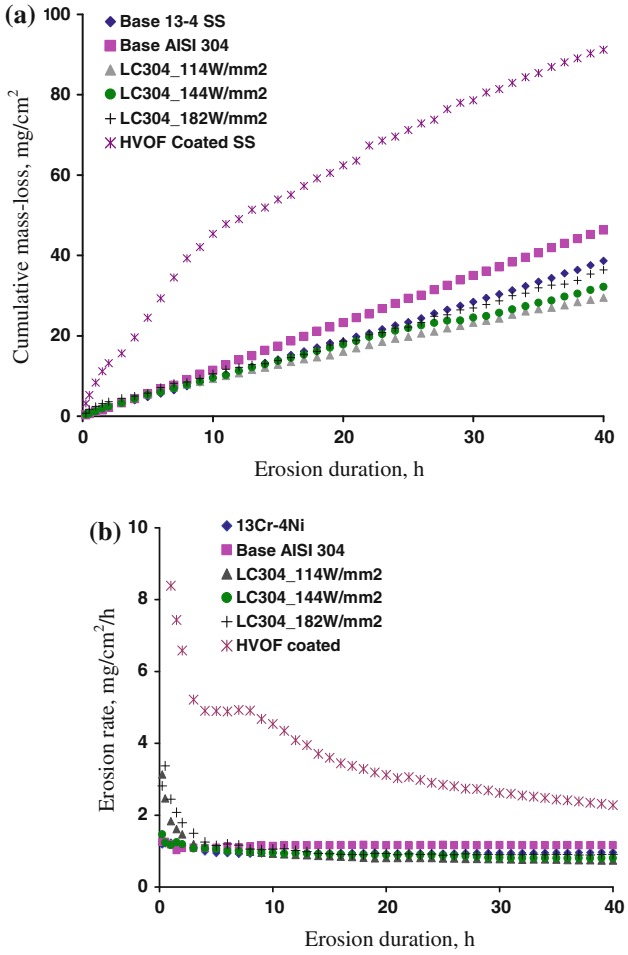

Fig. 6 (a) Solid particle erosion of laser cladded and HVOF coated stainless steels (b) variation in the erosion rate with increase in time

cladded stainless steel at 114 W/mm^2. The initial erosion (below 4 h) is significantly higher for cladded stainless steel as compared to those without cladding which may be due to the large initial roughness on the cladded surface inherited from the laser melting pattern. The HVOF coated stainless steel shows several fold (>10 times) higher erosion rates than the laser cladded and base substrate, up to 10 h of experiments. This difference, however, was reduced further to 2-3 times at the end of 40th hour of erosion.

3.3 Erosion Mechanism

The ploughing and microcutting, typical of ductile material, have been found the main erosion mechanisms operative in both the untreated AISI 304 and 13Cr-4Ni as shown in Fig. 7. The figure indicates the occurrence of uniform erosion on the surface of stainless steel. The untreated stainless steels undergo plastic deformation followed by microcutting due to hard alumina particles. The continued impact of alumina on the substrate resulted into the formation of craters and lips on the periphery. The removal of lips, during the subsequent particle jet, caused mass loss while crater formation enhanced the roughness on the material's surface. As opposed to the untreated substrate, the laser cladded surface revealed localized erosion marks as illustrated in Fig. 8. The area marked by 'A' has features closely resembles with the untreated surface while the area marked by 'B' shows distinct features showing particle-like shapes (tungsten carbide) which are intact to the surface. This indicates that the tungsten carbide particle did not suffer from erosion/wear. The base substrate below the clad was accessed and eroded (by the alumina jet) through the pores or cracks in the clad. It, thus, has dug out and loosen the tungsten carbide resulted into the mass loss. Erosion of the cladded surface, therefore, primarily appears due to the detachment of tungsten carbide particles subsequent to the erosion of the base substrate.

3.4 Corrosion Behavior

An OCP versus time plot for untreated and laser cladded stainless steels in 3.5% NaCl solution is shown in Fig. 9. A lower (more negative) OCP of the WC cladded as compared to that of the untreated stainless steels is apparent from the figure. The OCPs exhibited by the specimens laser cladded at 114 and 144 W/mm^2 are similar (~ -461 mV) but it is more active than the OCP of untreated 13Cr-4Ni and AISI 304 stainless steels (-98 and -131 mV, respectively). This indicates that the variation in laser power densities do not influence the oxide film forming mechanism under the freely corroding conditions (without impressing the potential/current). On comparing with the OCP of Co ~ -310 mV and WC $\sim +200$ mV (with respect to Ag/AgCl reference electrode) (constitutes of clad) in 3.5% NaCl solution (Ref 20), laser cladded shows more active potentials. More active ($-$ve) OCP of 83WC-17Co than that of the pure WC and cobalt indicates selective corrosion of Co instead of

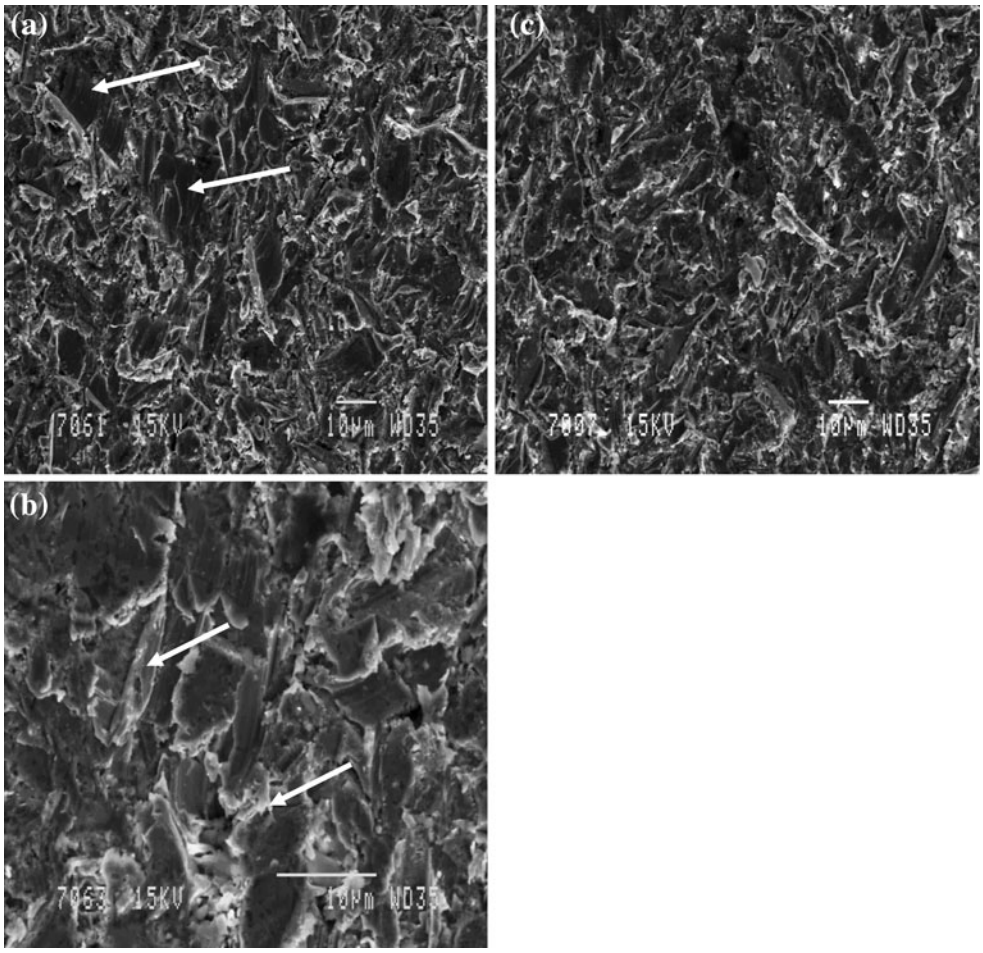

Fig. 7 Morphology after 20 h of erosion of untreated (a) 13Cr-4Ni (arrow shows craters) (b) 13Cr-4Ni at higher magnification (arrow shows lips) (c) AISI 304

WC (Ref 20). Active corrosion rate of Co has been reported to be faster when alloyed with the tungsten carbide as compared to that without WC alloying (Ref 21). This may be due to relative inertness of WC (being a ceramic material), thus resulting into the galvanic corrosion of Co when alloyed as Co-WC. This may further be seen from the schematic illustrated in Fig. 10. The values of electrochemical potential assigned in the Fig. 10 are based on the standard half cell reaction of Fe/Fe^{++}, Co/Co^{++}, and $WC + 5H_2O \rightarrow WO_3 + CO_2 + 10H^+ + 10e$ (Ref 22).

Figure 10 shows the galvanic current, $i_{WC\text{-}Co}$, from Co-WC couple is higher than from the cobalt alone, i_{Co}. Cobalt is anodic with respect to WC in a Co-WC couple. A more active OCP of HVOF coated (~ -561 mV) than the laser cladded and untreated stainless steels indicates acceleration of galvanic corrosion is likely under such circumstances. The OCPs were also recorded in the tap water and found to be similar to those observed in the NaCl solution. The untreated AISI 304 showed ~ -131 mV while those cladded at laser power densities $\sim$144 and 159 W/mm^2 showed ~ -455 and -443 mV, respectively. The OCP values of Co-WC obtained in the present study seems within the limit as equilibrium potential $E_{(Co(OH)_2/Co)} = -0.534$ V versus SCE at pH 6.8 by considering the following reaction (Ref 22)

$$Co + 2H_2O \rightarrow Co(OH)_2 + 2H^+ + 2e,$$
$$E_o = 0.11\,V/SHE\ (-0.132\ vs\ SCE).$$

The value of $E_{(Co(OH)_2/Co)}$ may, however, be influenced by the presence of chloride ions thereby change in the redox potential that results into the OCP values obtained as above.

Various electrochemical parameters of stainless steel 13Cr-4Ni and AISI 304 with and without laser cladding in NaCl and tap water are presented in Table 2. In NaCl solution, corrosion rate of laser cladded stainless steels is higher by about 2-3 times and HVOF coated is $\sim$210 times the untreated stainless steels. The difference in the corrosion rate of laser cladded and untreated is widened further in the tap water. The anodic polarization behavior of stainless steels, before and after the laser cladding, in both tap water and NaCl solutions are presented in Fig. 11(a) and (b). Stainless steels AISI 304 and 13Cr-4Ni in tap water demonstrate passivation; contrary to the laser cladded or HVOF coated specimens which suffer from active corrosion. The pitting potential (E_{pit}) of untreated AISI 304 is $\sim$+53 mV, indicating that it is resistant to pitting corrosion at OCP. Stainless steel 13Cr-4Ni seems to suffer from the pitting corrosion in NaCl solution as its OCP lies in the transpassive zone. The higher pitting potential, generally, indicates better resistance of alloy to pitting corrosion. The E_{pit} values of AISI 304 and 13Cr-4Ni in tap water are $\sim$1090 and 631 mV, respectively, much higher than those in the NaCl solution. This is due to the presence of higher chloride concentration ($\sim$35,000 ppm) in NaCl solution than in the tap

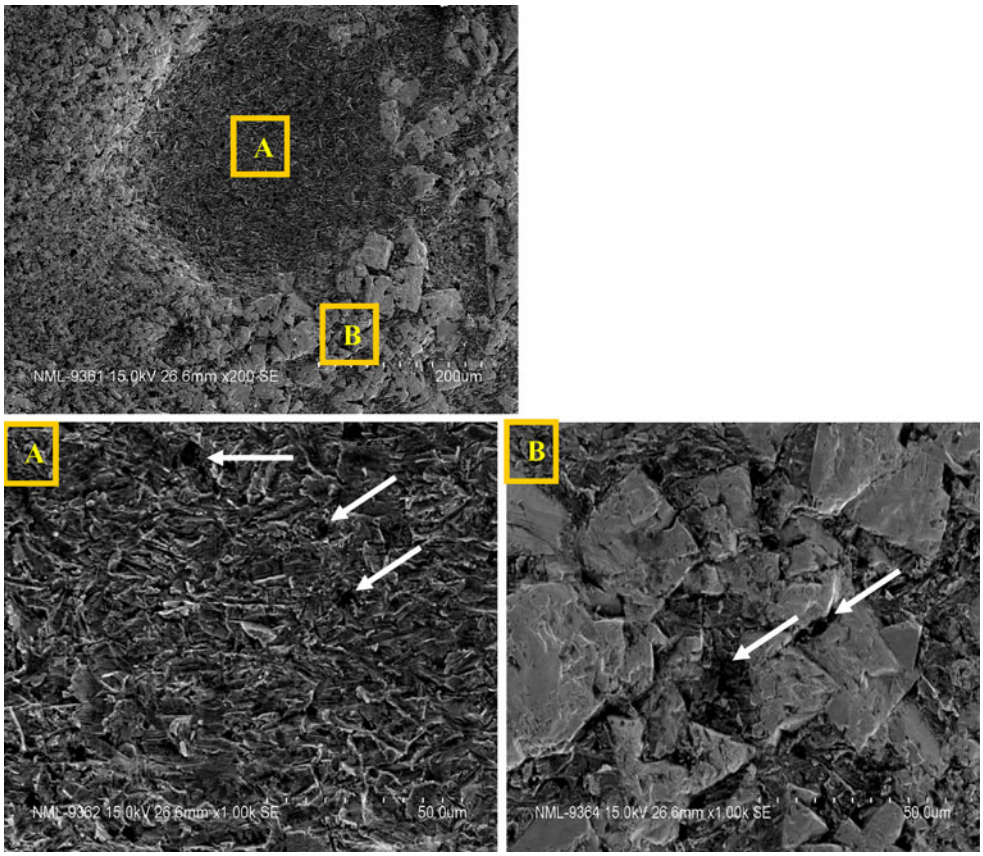

Fig. 8 Surface topography of laser cladded stainless steel after 40 h erosion ('A' and 'B' are magnified view of marked regions). Arrows in 'A' and 'B' show pores and cracks, respectively

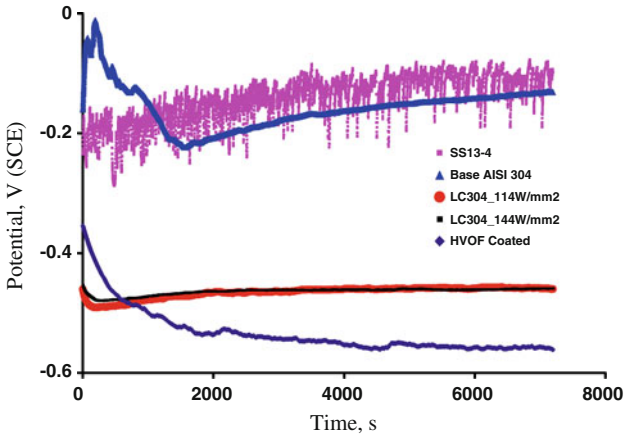

Fig. 9 Variation in OCP of the laser cladded stainless steel

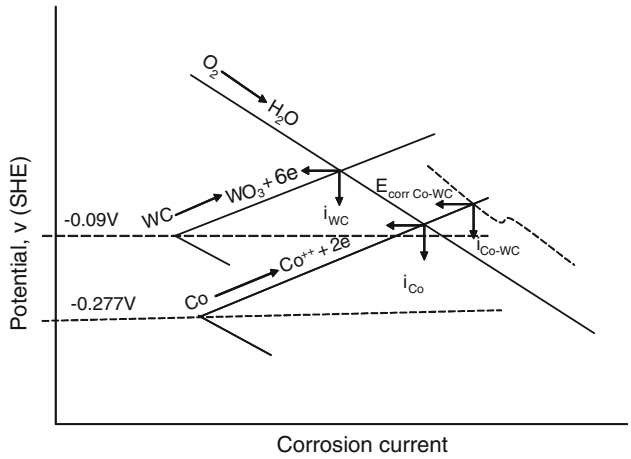

Fig. 10 Schematic showing galvanic corrosion between Co and WC

water (~50 ppm). The laser cladded and HVOF coated stainless steels did not show a passivation zone in the tap water where Cl^- concentration is significantly low. The results demonstrated an active corrosion of Co-WC laser cladded or HVOF coated stainless steel and the formation of protective passive film is difficult in both tap water and NaCl solution. Ceramics such as tungsten carbide are generally considered to be an inert and provide corrosion resistance in several environments by forming a barrier for ingress of corrosive species to the underlying surface. A report has shown that the WC electrode, prepared by hot pressing the powder, exhibited quasi-passive and pure cobalt yielded actively corroding behavior (Ref 20). Contrarily, Metikos et al. (Ref 23) showed passivation of pure cobalt in Hank's solution which contains ~8 g/L NaCl. Laser cladded or HVOF coated stainless steel, however, do not show barrier or quasi-passive nature as evident from the anodic polarization behavior (Fig. 11). The low cobalt content (17%) and pores in the laser clad seem responsible for

Table 2 Electrochemical parameters for stainless steel with and without laser cladding

Specimen designation	3.5% NaCl solution			Tap water		
	E_{corr}, mV	Corrosion rate, mpy	E_{pit}, mV	E_{corr}, mV	Corrosion rate, mpy	E_{pit}, mV
13Cr-4Ni	−79.9	1.32×10^{-2}	NIL	−107.6	7.88×10^{-3}	+631
AISI 304	−155.2	7.32×10^{-2}	+53	−146.4	8.95×10^{-3}	+1090
LC304_114 W/mm^2	−483.6	1.458	…	NT	NT	NT
LC304_144 W/mm^2	−470.6	2.585	…	−466.8	3.59	…
LC304_159 W/mm2	NT	NT	NT	−448.8	4.16	…
HVOF coated AISI 304	−561.3	15.34	…	−396.8	3.54	…

NA indicates not tested

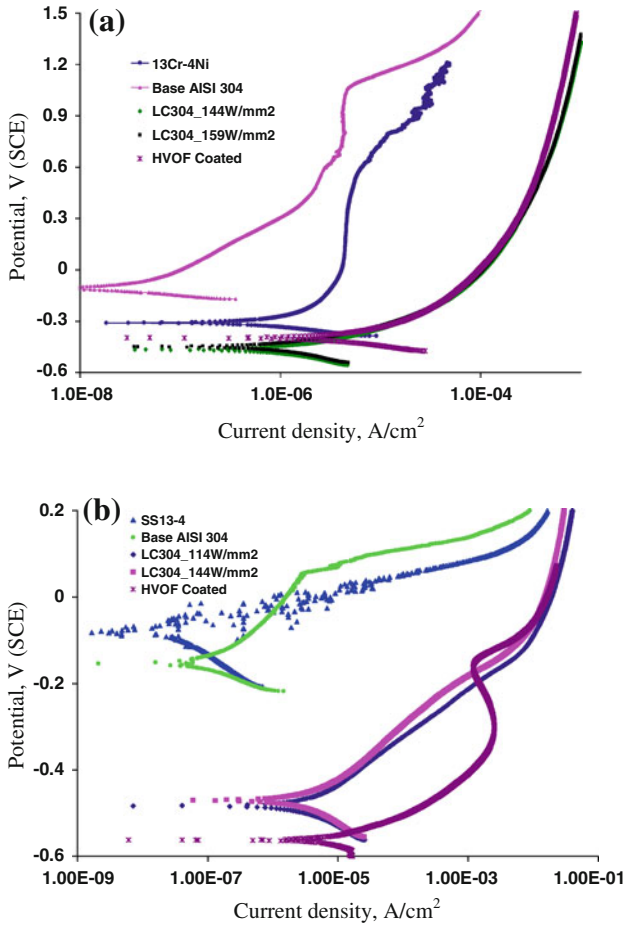

Fig. 11 Anodic polarization of untreated and laser treated stainless steels in (a) tap water (b) 3.5% NaCl solution

the active corrosion of stainless steel. The Co content in the laser cladded stainless steels may not be sufficient to provide an impermeable $Co(OH)_2$ oxide film which is responsible for the passivation. Pores in the clad further created unfavorable area ratio between cathode and anode and accelerated the corrosion of underlying substrate. Galvanic coupling between Co and WC in the clad or between WC and stainless steel at the bottom of the pores further enhanced the corrosion. In such situations, Co or stainless steel may be corroded preferentially. Selective leaching of cobalt from the cermet containing Co and tungsten carbide has shown responsible for higher corrosion rate (Ref 23). Corrosion of Co-WC was reported to increase with the increase in Co contents from 6 to 11% (Ref 24). Variation in laser power from 114 to 182 W/mm^2 did not change the anodic polarization behavior of laser cladded specimens. This is due to the fact that the corrosion in Co-WC is governed by the galvanic corrosion of Co and thus protected WC in the clad.

4. Conclusions

Laser cladding with Co-WC precursor has improved the hardness and erosion behavior of surface of stainless steel; the hardness of AISI 304 was increased by more than 3 times while that of the 13Cr-4Ni by about 2.5 times the hardness of untreated counterparts. The highest erosion resistance was observed at a laser power density of 114 W/mm^2, the erosion rate at this power density was ~0.74 mg/cm^2/h as compared to ~1.16 and 0.97 mg/cm^2/h for untreated AISI 304 and 13Cr-4Ni, respectively. The erosion of laser cladded stainless steel occurred due to detachment of WC particles. Corrosion resistance of the laser cladded stainless steels was significantly reduced. The laser cladding was found to hinder the passivation in AISI 304 stainless in both 3.5% NaCl solution and tap water. Both the stainless steels after laser cladding experienced an active corrosion.

Acknowledgments

The work carried out in this paper is part of a supra institutional project SIP0025. Help rendered by Shri Rajesh Jha in carrying out some laser cladding and erosion experiments is sincerely acknowledged.

References

1. G.I. Nikitenko, Studies to Reduce Cavitation Erosion of the Impellers in the Hydro Turbines at the Sayano-Shushenskoe Hydroelectric Plant, *Hydrotech. Construct.*, 1998, **32**, p 570–573
2. C.J. Heathcock, B.E. Protheroe, and A. Ball, Cavitation Erosion of Stainless Steels, *Wear*, 1982, **81**, p 311–327
3. R. Singh, S.K. Tiwari, and S.K. Mishra, Cavitation Erosion in Hydraulic Turbine Components and Mitigation by Coatings: Current Status and Future Needs, *J. Mater. Eng. Perform.*, 2012. doi:10.1007/s11665-011-0051-9
4. D.H. Graham and A. Bell, Particle Erosion of Candidate Materials for Hydraulic Valves, *Wear*, 1989, **133**, p 125–132
5. B.S. Mann and V. Arya, HVOF Coating and Surface Treatment for Enhancing Droplet Erosion Resistance of Steam Turbine Blades, *Wear*, 2003, **254**, p 652–668
6. D. Toma, W. Brandl, and G. Marginean, Wear and Corrosion Behaviour of Thermally Sprayed Cermet Coatings, *Surf. Coat. Technol.*, 2001, **138**, p 149–158

7. Y.P. Kathuria, Some Aspects of Laser Surface Cladding in the Turbine Industry, *Surf. Coat. Technol.*, 2000, **132**, p 262–269
8. F.T. Cheng, C.T. Kwok, and H.C. Man, Laser Surfacing of SS31603 Stainless Steel with Engineering Ceramics for Cavitation Erosion Resistance, *Surf. Coat. Technol.*, 2001, **139**, p 14–24
9. P. Wu, H.M. Du, X.L. Chen, Z.Q. Li, H.L. Bai, and E.Y. Jian, Influence of WC Particle Behavior on the Wear Resistance Properties of Ni-WC Composite Coatings, *Wear*, 2004, **257**, p 142–147
10. M. Riabkina-Fishman, E. Rabkin, P. Levin, N. Frage, M.P. Dariel, A. Weisheit, R. Galun, and B.L. Mordike, Laser Produced Functionally Graded Tungsten Carbide Coatings on M2 High-Speed Tool Steel, *Mater. Sci. Eng. A*, 2001, **302**, p 106–114
11. J. Przybyłowicz and J. Kusiński, Structure of Laser Cladded Tungsten Carbide Composite Coatings, *J. Mater. Process. Technol.*, 2001, **109**, p 154–160
12. C.P. Paul, H. Alemohammad, E. Toyserkani, A. Khajepour, and S. Corbin, Cladding of WC-12 Co on Low Carbon Steel Using a Pulsed Nd:YAG Laser, *Mater. Sci. Eng. A*, 2007, **464**, p 170–176
13. Y. Yang and H.C. Man, Microstructure Evolution of Laser Clad Layers of W-C-Co Alloy Powders, *Surf. Coat. Technol.*, 2000, **132**, p 130–136
14. M. Zhong, W. Liu, Y. Zhang, and X. Zhu, Formation of WC/Ni Hard Alloy Coating by Laser Cladding of W/C/Ni Pure Element Powder Blend, *Int. J. Refract. Met. Hard Mater.*, 2006, **24**, p 453–460
15. A. Hidouci, J.M. Pelletier, F. Ducoin, D. Dezert, and R. El Guerjouma, Microstructural and Mechanical Characteristics of Laser Coatings, *Surf. Coat. Technol.*, 2000, **123**, p 17–23
16. K. Van Acker, D. Vanhoyweghen, R. Persoons, and J. Vangrunderbeek, Influence of Tungsten Carbide Particle Size and Distribution on the Wear Resistance of Laser Clad WC/Ni Coatings, *Wear*, 2005, **258**, p 194–202
17. H. Chen, C. Xu, J. Qu, I.M. Hutchings, P.H. Shipway, and J. Liu, Sliding Wear Behaviour of Laser Clad Coatings Based Upon a Nickel-Based Self-Fluxing Alloy Co-deposited with Conventional and Nanostructured Tungsten Carbide-Cobalt Hardmetals, *Wear*, 2005, **259**, p 801–806
18. V.K. Nanda, Parameters Affecting Abrasion and Remedial Measures, *Proceedings of 1st International Conference on Silting Problems in Hydro Power Plants*, 1999, New Delhi, India, p 43–52
19. H.S. Sidhu, B.S. Sidhu, and S. Prakash, Solid Particle Erosion of HVOF Sprayed NiCr and Stellite-6 Coatings, *Surf. Coat. Technol.*, 2007, **202**, p 232–238
20. C. Monticelli, A. Frignani, and F. Zucchi, Investigation on the Corrosion Process of Carbon Steel Coated by HVOF WC/CO Cermets in Neutral Solution, *Corros. Sci.*, 2004, **46**, p 1225–1237
21. A.M. Human and H.E. Exner, The Relationship Between Electrochemical Behaviour and In-Service Corrosion of WC Based Cemented Carbides, *Int. J. Refract. Met. Hard Mater.*, 1997, **15**, p 65–71
22. J.D. Voorhies, Electrochemical and Chemical Corrosion of Tungsten Carbide (WC), *J. Electrochem. Soc.*, 1972, **119**, p 219–222
23. M. Metikos-Hukovic and R. Babic, Passivation and Corrosion Behaviors of Cobalt and Cobalt-Chromium-Molybdenum Alloy, *Corros. Sci.*, 2007, **49**, p 3570–3579
24. W.J. Tomlinson and C.R. Linzell, Anodic Polarisation and Corrosion of Cemented Carbides with Cobalt and Nickel Binders, *J. Mater. Sci.*, 1988, **23**, p 914–918